Journal of Structural Geology 33 (2011) 970–984

Contents lists available at ScienceDirect

Journal of Structural Geology

journal homepage: www.elsevier.com/locate/jsg

Structure and evolution of a rocksalt-mudrock-tectonite: The haselgebirge in the Northern Calcareous Alps

Christoph Leitner [a,*], Franz Neubauer [a], János L. Urai [b], Johannes Schoenherr [c]

[a] Fachbereich für Geographie und Geologie, Universität Salzburg, Hellbrunnerstraße 34, 5020 Salzburg, Austria
[b] Geologie-Endogene Dynamik, RWTH Aachen, Lochnerstraße 4-20, 52056 Aachen, Germany
[c] Exxon Mobil Upstream Research Company, Carbonate Reservoir Performance Prediction, 3319 Mercer Street, Houston, TX 77027, USA

ARTICLE INFO

Article history:
Received 7 June 2010
Received in revised form
1 February 2011
Accepted 18 February 2011
Available online 9 March 2011

Keywords:
Haselgebirge
Rocksalt
Halite
Hydrofracturing of mudrock
Northern Calcareous Alps
Alps

ABSTRACT

The Northern Calcareous Alps are part of the Eastern Alps in Austria and Germany. The Mesozoic units of this fold-and-thrust belt were detached, thrusted and stacked along the evaporitic Haselgebirge Formation. Exposed in salt mines, rocksalt and mudrock form a two component tectonite: The rock type "haselgebirge" consists of 10–70 wt % halite with silt- to gravel- or block-sized components within a halite matrix, and the "kerngebirge" with >70 wt % halite. All rock types studied are fault rocks. By use of a temperature-independent subgrain size piezometer, the paleo-differential stress of halite was calculated at ca. 2.5 MPa in Altaussee and ca. 4.5 MPa in Berchtesgaden. Including data from a grain-size piezometer, temperatures were estimated at ca. 150 ± 20 °C and 110 ± 10 °C. This implies very high strain rates, which are about 10^{-10}–10^{-9} s^{-1}. During the tectonic movement, the halite deformed, recrystallized, and crystallized as veins in mudrock fractures. We interpret high overpressure of the pore fluid to have significantly contributed to fracturing of the mudrock.

1. Introduction

Formations comprising rocksalt or other evaporites at the basis of thrusted cover units exist for instance, in the Appalachians (Davis and Engelder, 1985), Swiss Jura (Sommaruga, 1999), the Salt Range in Pakistan (Jadoon and Frisch, 1997) and in the Zagros Mountains (Alavi, 2007). The taper of salt thrust wedges may be very small (≈1°), providing shallow overthrusts (Davis and Engelder, 1985). The Northern Calcareous Alps (NCA, Fig. 1a) form a fold-and-thrust belt within the Austroalpine unit of the Austrian Eastern Alps. The rheologically weak evaporitic series at the base acted as one of the major detachment levels of nappes in high structural levels within NCA (e.g. Linzer et al., 1995).

The Haselgebirge Formation (Buch, 1802) is an evaporitic succession, which was formed as a rift sequence close to the lithostratigraphic base of the NCA succession. Operating salt mines provide subsurface exposures, where the salt has been mined in central sectors of the Northern Calcareous Alps (Salzkammergut, Fig. 1a–b) for more than 3000 years (Stöllner, 2003; Klein, 2006; Grabner et al., 2007). Halite, mudrock and subordinate anhydrite and polyhalite form an evaporitic mélange (Schauberger, 1931, 1949, 1986). The foliation visible in underground mines was first interpreted as sedimentary (Schauberger, 1953), but structures pointing to ductile deformation and folds combined with brittle deformation of the mudrock suggested a tectonic origin of the layering (Mayerhofer, 1955; Spötl, 1989a). The average halite content ranges between ca. 30–65 vol % (Schauberger, 1986). This rock type is called "haselgebirge" (nomenclature after Schauberger, 1986).

The central sectors of the Northern Calcareous Alps underwent strong diagenetic modifications to low-grade metamorphic conditions during the Late Jurassic to early Late Cretaceous. Maximum temperatures at around 200–300 °C were estimated (Kralik et al., 1987; Spötl, 1992; Götzinger and Grum, 1992; Gawlick et al., 1994; Wiesheu and Grundmann, 1994; Spötl et al., 1996, 1998a, 1998b; Wiesheu, 1997; Spötl and Hasenhüttl, 1998; Rantitsch and Russegger, 2005). Maximum temperatures increase towards the south, while cooling ages get younger towards the southern margin. Age estimates for this thermal peak range between 150 Ma and 90 Ma (Kirchner, 1980; Kralik et al., 1987; Hejl and Grundmann, 1989; Götzinger and Grum, 1992; Gawlick et al., 1994; Spötl et al., 1996, 1998a, 1998b; Gawlick and Höpfer, 1996; Rantitsch and Russegger, 2005; Frank and Schlager, 2006).

The aim of this study is to constrain the conditions and the mechanisms by which the haselgebirge developed. Underground

* Corresponding author. Tel.: +43 662 8044 5400; fax: +43 662 8044 621.
E-mail address: christoph.leitner@sbg.ac.at (C. Leitner).

0191-8141/$ – see front matter © 2011 Elsevier Ltd. All rights reserved.
doi:10.1016/j.jsg.2011.02.008

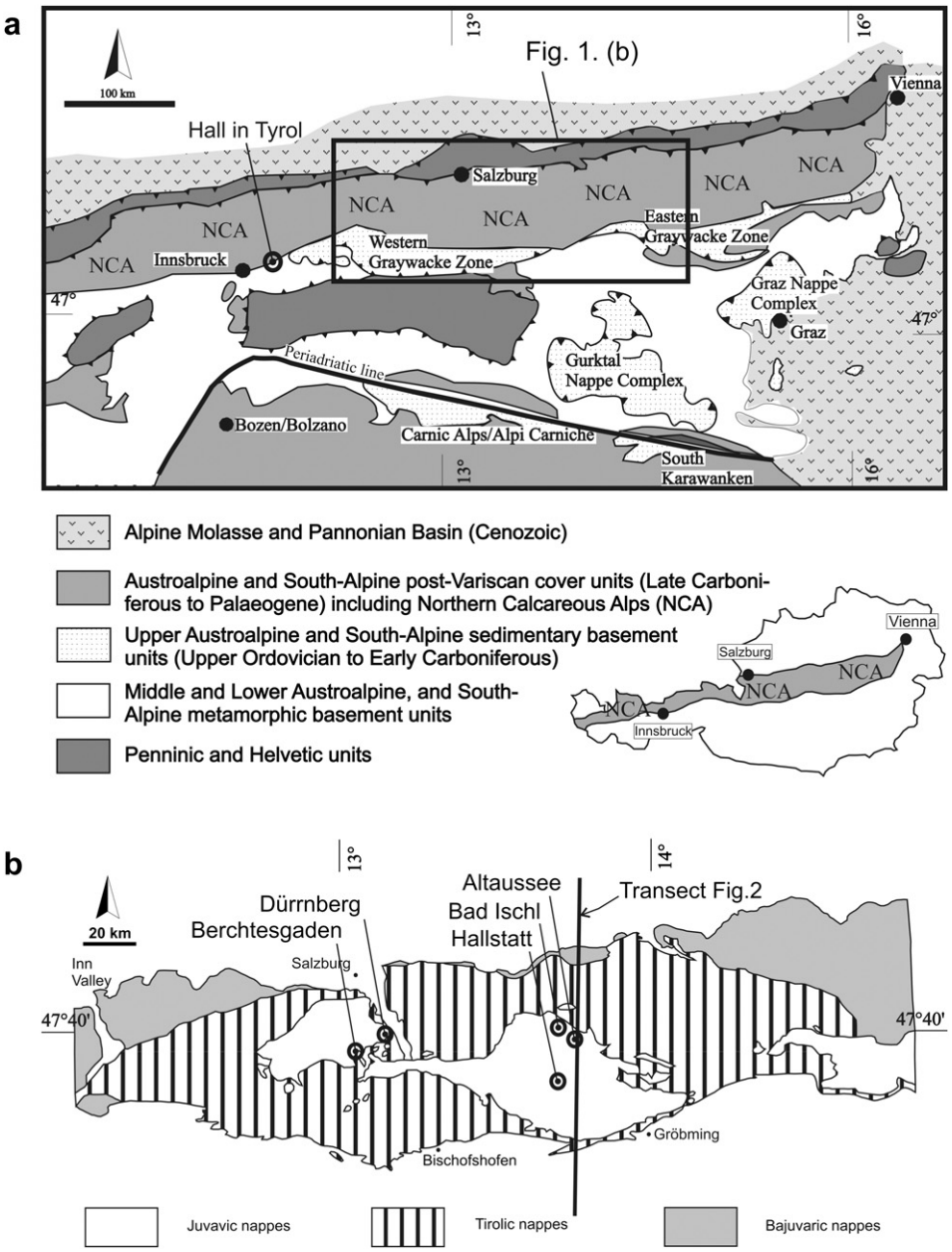

Fig. 1. (a) Overview of the Eastern Alps. Main tectonic units and location of the NCA. Insert at right bottom gives the position within Austria. (b) Fold-and-thrust belt of the central Northern Calcareous Alps, based on Oberhauser (1980). Circles mark rocksalt deposits.

observations were combined with thin section analysis, and paleostress and strain rate were calculated using experimental calibrations.

2. Mechanical behaviour of rocksalt and mudrock

In the following, "halite" is used as the name of the mineral, "rocksalt" refers to the monomineralic rock of halite with only minor xenolithic inclusions, "salt rock" refers to rocks with various halite contents and "salt" is an undifferentiated expression.

Piezometers relate subgrain and grain size and differential stress during deformation. The piezometer for halite (Carter et al., 1993; Schléder and Urai, 2005, 2007) relates differential stress to the steady-state subgrain size in halite:

$$D = 215\sigma^{-1.15} \quad (1)$$

where D is the average diameter of the subgrains and σ is the differential stress. It is almost temperature-independent. The new piezometer of Ter Heege et al. (2005) relates the actual grain size to differential stress and temperature. Armann (2008) observed the evolution of different grain sizes by recovery processes during deformation in simple shear experiments.

A creep law relates differential stress and strain rate. For rocksalt, deformation by dislocation creep the strain rate $\dot{\varepsilon}$ can be related to the flow stress ($\Delta\sigma$) using a power law creep equation:

$$\dot{\varepsilon} = A \exp(-Q/RT)\Delta\sigma^n \quad (2)$$

where the pre-exponential constant A has the dimensions M Pa^{-n} s^{-1}, Q is the apparent activation energy for creep in J mol^{-1}, R is the gas constant in J mol^{-1} K^{-1}, T is the temperature in °K, $\Delta\sigma = \sigma_1 - \sigma_3$ is the differential stress in MPa and n is the dimensionless stress exponent. Extrapolation is only valid, if the deformation

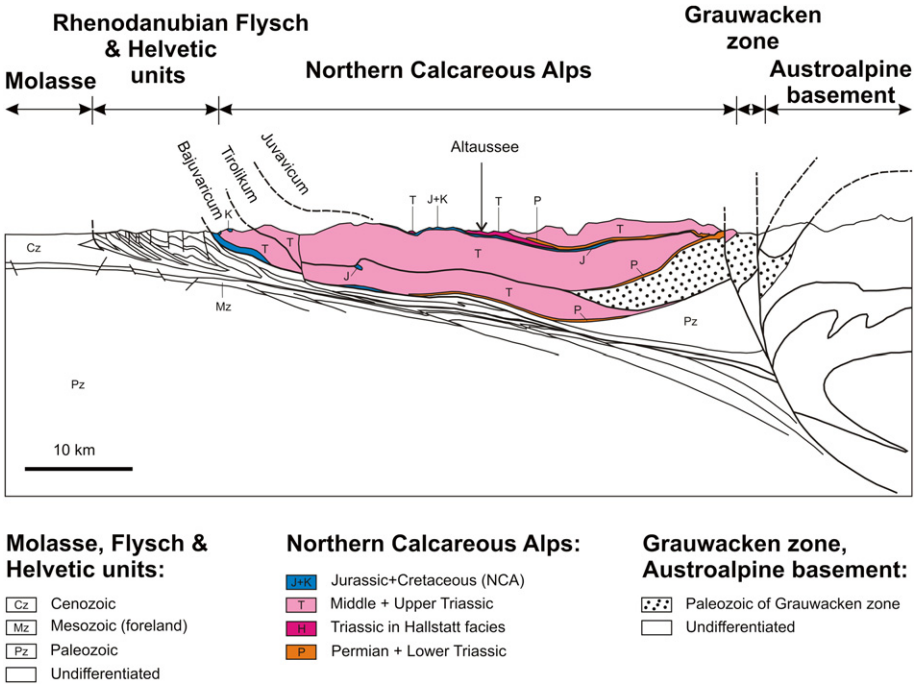

Fig. 2. Geological transect of the central NCA (modified after Schmid et al., 2004).

mechanisms remain the same in experiment and in nature. Several studies on natural halite indicate that, at geological strain rates, salt is in the transition regime where both dislocation creep and solution-precipitation creep mechanisms operate:

$$\dot{\varepsilon} = \dot{\varepsilon}_{DC} + \dot{\varepsilon}_{PS} \tag{3}$$

(Spiers and Carter, 1998; Urai et al., 2008)

$$\dot{\varepsilon}_{DC} = 8.1 \times 10^{-5} \exp(-51600/RT)\Delta\sigma^{3.4} \tag{4}$$

(Carter et al., 1993)

$$\dot{\varepsilon}_{PS} = 4.7 \times 10^{-4} \exp(-24530/RT)\ \Delta\sigma/TG^{3} \tag{5}$$

(Spiers et al., 1990)

G is the grain size diameter in mm.

Water weakening of ductile rock is usually related to intracrystalline effects on dislocation mobility or lattice diffusion, or intercrystalline effects such as enhanced grain boundary diffusion, enhanced grain boundary sliding, or solution-precipitation effects (e.g. Ter Heege et al., 2005). The content of fluid inclusions is 1–2 vol % in original bedded pure halite salt (Roedder, 1984). In naturally deformed samples, brine is present in fluid inclusions along grain boundaries. Synthetic rocksalt shows differences in deformation mechanisms, depending on whether it is "wet" (>20 ppm) or "dry" (<10 ppm) (Trimby et al., 2000a). In wet mobile grain boundaries, a fluid film was proposed with a thickness of <50 nm (Schenk and Urai, 2004, 2005; de Meer et al., 2005). Permeability of natural rocksalt is around $K = 10^{-20}$ m (e.g. Lux, 2005; Peach and Spiers, 1996). Compared with other rock types, rocksalt contains only trace amounts of water, but for halite this enhances fluid-assisted grain-boundary migration and pressure solution.

The nature of the relation between the effective stress, differential stress and permeability was studied in a series of experiments (Urai et al., 1986; Peach and Spiers, 1996; Peach et al., 2001; Popp et al., 2001). The permeability of rocksalt increases by five orders of magnitude if deformed at low temperatures and mean

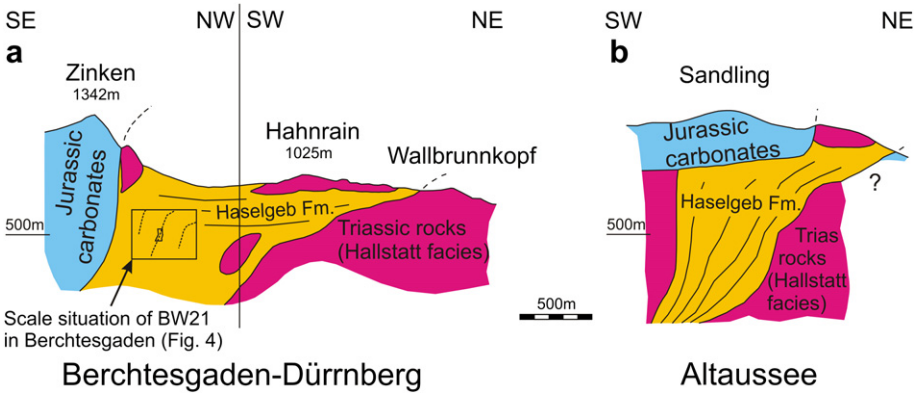

Fig. 3. (a, b) Cross sections through the salt bodies of Berchtesgaden (after Plöchinger, 1996) and Altaussee. Lines in salt rock mark orientation of foliation and salt layers (compare Fig. 4).

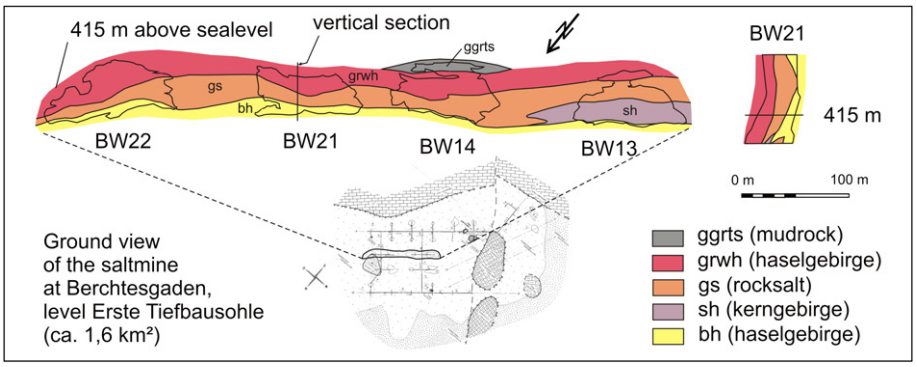

Fig. 4. Berchtesgaden mine. Thick salt layers can be traced through leach caverns. Overview from Kellerbauer (1996); abbreviations: ggrts - grüngrauer Tonstein, grwh - rötlich grünes Haselgebirge, gs - graues Kernsalz, sh - Kerngebirge, bh- buntes Haselgebirge (Schauberger, 1986).

effective stress due to microcracking and dilatancy. Similar dilatancy was reported for sealed liquid-filled salt cavities by Lux (2005), who noted that diffuse dilatancy occurs with dilated grain boundaries when the fluid pressure slightly exceeds σ_3, while hydrofracturing occurs when the fluid pressure significantly exceeds σ_3. Under the mentioned conditions, water is expelled from the salt rock. Natural occurrence of diffuse dilatancy was reported in rocksalt samples from the vicinity of oil fields of the Oman salt basin (Schoenherr et al., 2007a). Oil was entrapped along cleavage planes in halite and at grain boundaries. In the presence of high fluid pressure the effective stress was decreased so that dilatancy was reached. After pressure reduction the infiltration stopped. A different process, leading to increased permeability of salt was reported by Lewis and Holness (1996). The contact angle between halite and brine is 70°. This leads to the closure of grain boundaries by halite precipitation in laboratory conditions (Schenk and Urai, 2004). Lewis and Holness measured the equilibrium water-halite dihedral angles in grain boundary triple junctions. At temperatures $<$100 °C these were higher than 60°, so that the small amounts of brine present in the salt are distributed in micrometer-sized isolated fluid inclusions. At temperatures $>$100 °C and pressures of 70 MPa this value decreases below 60°, leading to a redistribution of the fluid into a thermodynamically stable network of connected, fluid filled channels at grain boundary triple junctions. Peach and Spiers (1996) proposed that hydraulic fracturing or dilatancy of rocksalt could occur under low effective stress during natural deformation of rocksalt at great depth and high pore-fluid pressure.

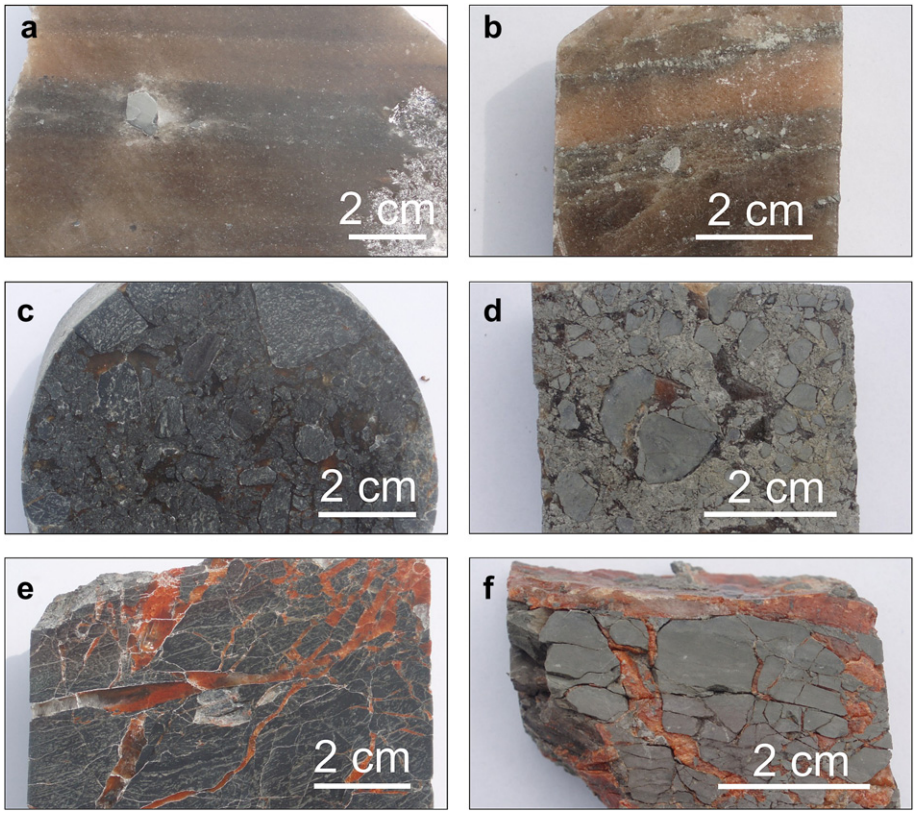

Fig. 5. (a, b) Nearly pure rocksalt with an ultramylonitic to mylonitic fabric, sample BDG-13. (c, d) Haselgebirge with a protocataclastic to cataclastic fabric, sample BDG-bh. (e, f) Mudrock with a low matrix content and a high degree of coherence of clasts, sample BDG-ts. In the series (a)-(c)-(e) the halite content diminishes from 100 via 40 to 10%, whereas the fitting of mudrock components increases from 0 via 10–90%.

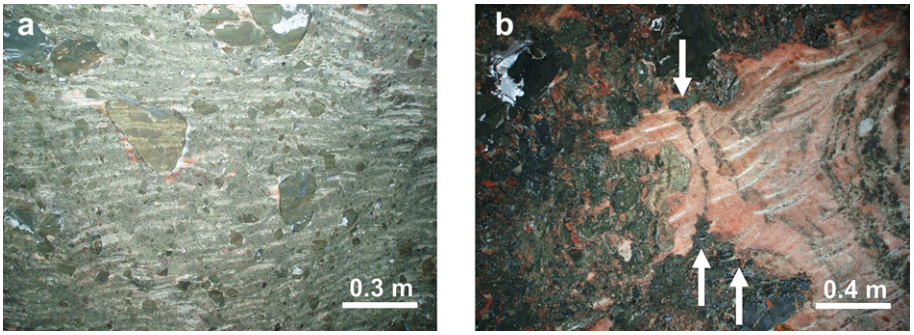

Fig. 6. (a) Typical mature haselgebirge. White horizontal streams from tunnel boring machine. (b) Cutout of a salt patch, dark lines are cut off by the surrounding haselgebirge, Berchtesgaden mine.

Besides the release of water from fluid inclusions, the fluids in rocksalt may be externally derived, from sedimentary successions underneath or lateral to the salt bodies. Alternatively, the fluids may be generated inside the salt body, e.g. by the gypsum-to-anhydrite conversion (Borchert and Muir, 1964). This reaction would result in a release of 40 vol % structural water. The carnallite-to-sylvite transition releases 40 vol % of water (Borchert and Muir, 1964). The porosity of mudrock/shale decreases rapidly with depth (Magara, 1980; Deng et al., 1996; Tucker, 1991). The release of water by the smectite to illite transition of mixed-layer clays (S-I-transition) is most sensitive to changes in temperature between 60 and 90 °C (e.g. Deng et al., 1996; Couzens-Schultz and Wiltschko, 2000; Charpentier et al., 2003; Saffer et al., 2008).

The system halite-water-mudrock has been shown to induce enhanced pressure solution of halite and hydrofracturing of mudrock. The strong influence of mudrock or other non-halite materials for solution-precipitation of halite has been stated in several experiments (Hickman and Evans, 1995; Martin et al., 1999; Schutjens and Spiers, 1999; Lohkämper et al., 2004).

3. Geological setting

3.1. The Northern Calcareous Alps

The classic division within the Northern Calcareous Alps defines the Bajuvaric, Tirolic and Juvavic nappe complexes (Figs. 1 and 2). Thrusting prograded from south to north (Linzer et al., 1995; Neubauer et al., 2000).

The age of formations in the Northern Calcareus Alps ranges from late Carboniferous or early Permian to Eocene. Rocksalt deposits are mostly found in the Lower Juvavic unit. The westernmost part of the expanding Triassic Tethys Ocean is called the Meliata ocean, which comprises rare deep-sea (ophiolitic?) sequences in the eastern parts of the NCA (Faupl and Wagreich, 2000; Neubauer et al., 2000). The Meliata Ocean was closed in the Late Jurassic (Dallmeyer et al., 2008). Coevally, the sea floor deepened on top of the subsiding lithosphere and reached maximum water depths in the footwall plate by thrust loading and radiolarites were deposited in the basin. Gravitational sliding is reported from various places (Tollmann, 1987; Mandl, 1982). From the Late Jurassic to Middle Cretaceous, nappe stacking of Austroalpine units started due to the subduction of the Austroalpine continental crust. The mechanism and the time of emplacement of the Juvavic units is still a matter of controversy. The classic hypothesis assumes that both Juvavic nappes took their position during the Eo-Alpine nappe tectonics (Mandl, 2000).

In the Eocene, the second stage of the Alpine orogeny occurred, resulting in the collision of the stable European continent with the overriding Austroalpine units. The Northern Calcareous Alps as we know them today were detached from their basement and thrusted over the Rhenodanubian Flysch and Helvetic domain resulting in a wide thin-skinned tectonic nappe complex (Linzer et al., 1995; Neubauer et al., 2000). The detachment happened beneath the lowermost unit, the Bajuvaric nappe (Fig. 2). Deformation of Upper Cretaceous to Eocene Gosau basins deposited on the uppermost nappes (Tirolic and Juvavic nappes) suggests some last pulses of tectonism in this area in the late Eocene to early Miocene.

3.2. The salt mines of the Northern Calcareous Alps (Austria and Germany)

The underground mines of Berchtesgaden and Dürrnberg are located in the same salt body. At the surface, the body extends ca. 7 km, and is 0.5–2.0 km wide. It is at least 600 m thick (Kellerbauer, 1996). The body is squeezed between a lower Tirolic nappe and a higher Juvavic nappe (Pichler, 1963; Plöchinger, 1990, 1996; Braun, 1998; Gawlick and Lein, 2000; Figs. 3a and 4).

The Haselgebirge Formation body of Altaussee crops out around the mountain Sandling, 2.3 km on ground view, >1200 m thick (Medwenitsch, 1958; Proisl, 2003). The halite content of haselgebirge lies at 65% and it is typically red due to polyhalite. It comprises, and is bordered by, Triassic limestone, and Jurassic rocks cover the deposit (Fig. 3b).

The salt body of Hall in Tyrol lies between the lower Bajuvaric nappe and the higher Tirolic nappe and interpreted to be cut off with depth (Schmidegg, 1951; Oberhauser, 1980; Spötl, 1989b). The halite content is only around 30%. It comprises large bodies of

Table 1
Nomenclature of salt rocks after Schauberger (1986), simplified. On the right, the well-established structural classification of fault rocks.

Rock type (according to Schauberger, 1986)	Salt in wt %	In terms of textural classification of fault rocks (e.g. Wise et al., 1984)
Rocksalt (nearly pure)	100 – 90	Ultramylonite
Kerngebirge (rich in rock salt)	90 – 70	Mylonite
Haselgebirge (medium content of rock salt)	70 – 10	Protocataclasite, cataclasite, protomylonite, mylonite
Shale (deformed/ undeformed)	10 – 0	Crush breccia

Table 2
Salt rock samples for thin section analysis. ALT = Altaussee, BDG = Berchtesgaden, DÜ = Dürrnberg.

Sample	Location	Depth	Rock name	Meso-lithology
DÜ-4C	Wolf-Dietrich, next Leth Schacht	365 m	Haselgebirge	Grey mudrock, red+white halite
BDG-mbsh	TB-258, 192m, Keder-Brandstatt-Scholle	250 m	Kerngebirge	Black+red mudrock, polyhalite, red+white halite
BDG-gh	TB-258, 91m, Keder-Brandstatt-Scholle	200 m	Haselgebirge	Grey mudrock, subordinate polyhalite, red+white halite
BDG-ggrwh	TB-258, 231m, Keder-Brandstatt-Scholle	290 m	Haselgebirge	Grey+green+red mudrock, dark+white halite, subordinate polyhalite
BDG-bh	B-3, 3m, next BW84	300 m	Haselgebirge	Grey+black mudrock, anhydrite, red halite
BDG-bsh	B-4, 11m, next BW91	325 m	Kerngebirge	Grey mudrock, subordinate anhydrite+polyhalite, dark- red halite
ALT-3	Erbstollen, next to the planed cavern E6	525 m	Rocksalt	Halite with dark and red layers from fine mudrock and polyhalite
ALT-26	Blindhorizont, Brechwerk	370 m	Rocksalt	Halite, contaminated with mudrock and polyhlite particles
ALT-30	Franzberg, cross Jorkasch-Koch/Lemberg	335 m	Rocksalt	Halite, layers of red and dark colour from polyhalite/mudrock
ALT-37A	Franzberg, Danner Werk Ablass	380 m	Rocksalt	Red halite, contaminated with mudrock and polyhalite particles
ALT-39	Franzberg, Jorkasch-Koch, Flucht/Wetter	430 m	Rocksalt	Halite, blured layers of red and grey colour from polyhalite/mudrock
DÜ-7C	Untersteinberg, top of Backhaus Rolle	190 m	Rocksalt	Dirty red halite, nebulous, polyhalite and mudrock particles
DÜ-24A	Jabobberg, bottom of Haupolter Schurf	230 m	Rocksalt	Grey halite, from anhydrite and mudrock
DÜ-30	Obersteinberg, next Schiller Schurf	160 m	Rocksalt	Intense red halite, blurred layers, single pieces of mudrock
DÜ-41D	Georgenberg, Zubau Werk Nr.12	110 m	Rocksalt	Halite with dark and red streams from fine mudrock and polyhalite
BDG-10	BW22, 7.Vermessung (20.07.2006)	320 m	Rocksalt	Pure, clear halite, small euhedral anhydrite

dolomite-anhydrite rocks, which are dated as Lower Triassic (Spötl, 1988). In Bad Reichenhall, saturated brine is produced from boreholes, which were drilled down to 1200 m below groundlevel. Interestingly, there are also rocks of Paleogene age incorporated into the Haselgebirge (Schauberger et al., 1976). Around Bad Ischl, salt outcrops are rare and hidden by the overlying rocks. The salt is squeezed between Triassic, Jurassic and Cretaceous rocks (Medwenitsch, 1958; Mayerhofer, 1955). The salt body of Hallstatt extends ca. 3.0 km in an E-W direction, is 0.5 km broad, and >800 m thick (Habermüller, 2005; Arnberger, 2006). The halite content of haselgebirge is around 55% (Schauberger, 1931, 1949). Most incorporated rocks are limestones of the Hallstatt facies; red sandstones suggest a connection with the Southern Alps (Spötl, 1987). The covering mountain Plassen is of Jurassic age (Gawlick and Schlagintweit, 2006).

4. Methods

During this study, all the mines were visited (Fig. 1a–b). We prepared 10 samples from Berchtesgaden (BDG), 5 from Dürrnberg (DÜ) and 8 from Altaussee (ALT). Around one third were of haselgebirge from the Berchtesgaden mine (Table 2).

Samples for thin sections of rocksalt and haselgebirge were taken from underground galleries or drill cores. Slabs of 50 × 25 mm with a thickness of 25 mm were cut perpendicular to the foliation/bedding plane, parallel to the grain-shape preferred orientation (including lineation), using a water-cooled diamond saw to avoid microcracking in the geological laboratories of the Salzburg University, Austria (Schléder and Urai, 2005). In several cases, no lineation was visible. All samples were dried at 40 °C for two days afterwards to avoid further destruction of the mudrock. Samples were gamma-irradiated for 3 months at 100 °C with a dose rate between 4 and 6 kGy/h (kilograys per hour) to a total dose of about 4 MGy (megagrays) at the research reactor of the research center in Jülich, Germany, to decorate otherwise invisible microstructures. From unirradiated and irradiated samples, thin sections were prepared, using the method described by Urai et al. (1987) and Schléder and Urai (2005).

In all rocksalt samples, the halite crystals contain well-developed subgrains between 10 and 400 μm. For piezometry, photographs of subgrain structures were taken in reflected light. For the calculation of the subgrain area, the subgrain borders were traced with the computer program AutoCAD Civil 3D (Fig. 12, Fig. 13). The area data was used to calculate an equivalent circular diameter (ECD) for each subgrain. *D* was taken as the arithmetic mean of all subgrains in one sample (Schléder and Urai, 2005).

5. Results

5.1. Nomenclature of salt rocks from the Haselgebirge Formation

The nomenclature of Schauberger (1986) was developed for the mining practice with no genetic interpretation (Table 1). It classifies rocks by halite content and the colour of mudrock. For example "green red haselgebirge" means a content of 10–70 wt % rocksalt with green and red mudrock components. Below 20 wt % the rock is usually component-supported, while above 20 wt % it is matrix-supported (Kellerbauer, 1996). Mayerhofer (1955) and Spötl (1989a) interpreted the salt rocks of the Haselgebirge Formation to be of tectonic origin, but no structural classification was proposed.

We found that all of the salt rocks of the Haselgebirge Formation exposed in the mines of Altaussee, Berchtesgaden and Dürrnberg represent various types of fault rocks ranging from cataclasites to mylonites (Fig. 5a–f). Here, we juxtapose the nomenclature of Schauberger (1986) to the structural classification commonly used in structural geology (e.g., Wise et al., 1984). While all the rocksalt we observed was foliated, the mudrock was usually internally undestroyed. In terms of the structural classification of fault rocks, haselgebirge with up to 50 wt % halite is mainly protocataclasite. The higher the halite content, the more foliated the rock appears. The halite-rich kerngebirge is, therefore, always a mylonite in the structural classification (Table 1).

Sedimentologically, conglomerates and breccias are classified according to the relative proportion of rock fragments and matrix, as well as the degree of roundness and fitting of the detrital components. The amount of matrix is equal to the halite content in the case of the haselgebirge of Schauberger (1986). Fitting is described as the relative movement of clasts. On the basis of Richter and Füchtbauer (1981), we quantified the fitting as vol % of fitting clasts of the present clasts. According to the nomenclature of tectonic breccias after Richter and Füchtbauer (1981), haselgebirge is a "mélange".

5.2. Haselgebirge and rocksalt in underground mining

The salt rock exposes all types of transitions from nearly undeformed mudrock to nearly pure rocksalt. Haselgebirge can reach different stages of homogenisation or maturity. In a stage of high maturity, the mudrock components are not larger than equidimensional pieces of gravel (Deutsches Institut für Normung e.V., 2004; Fig. 6a). The matrix consists of red and white rocksalt. The components are often covered with a dark slickensided rim. Up to meter-sized clasts of anhydrite, polyhalite rock and mudrock are sometimes found within haselgebirge. These rocks often preserved

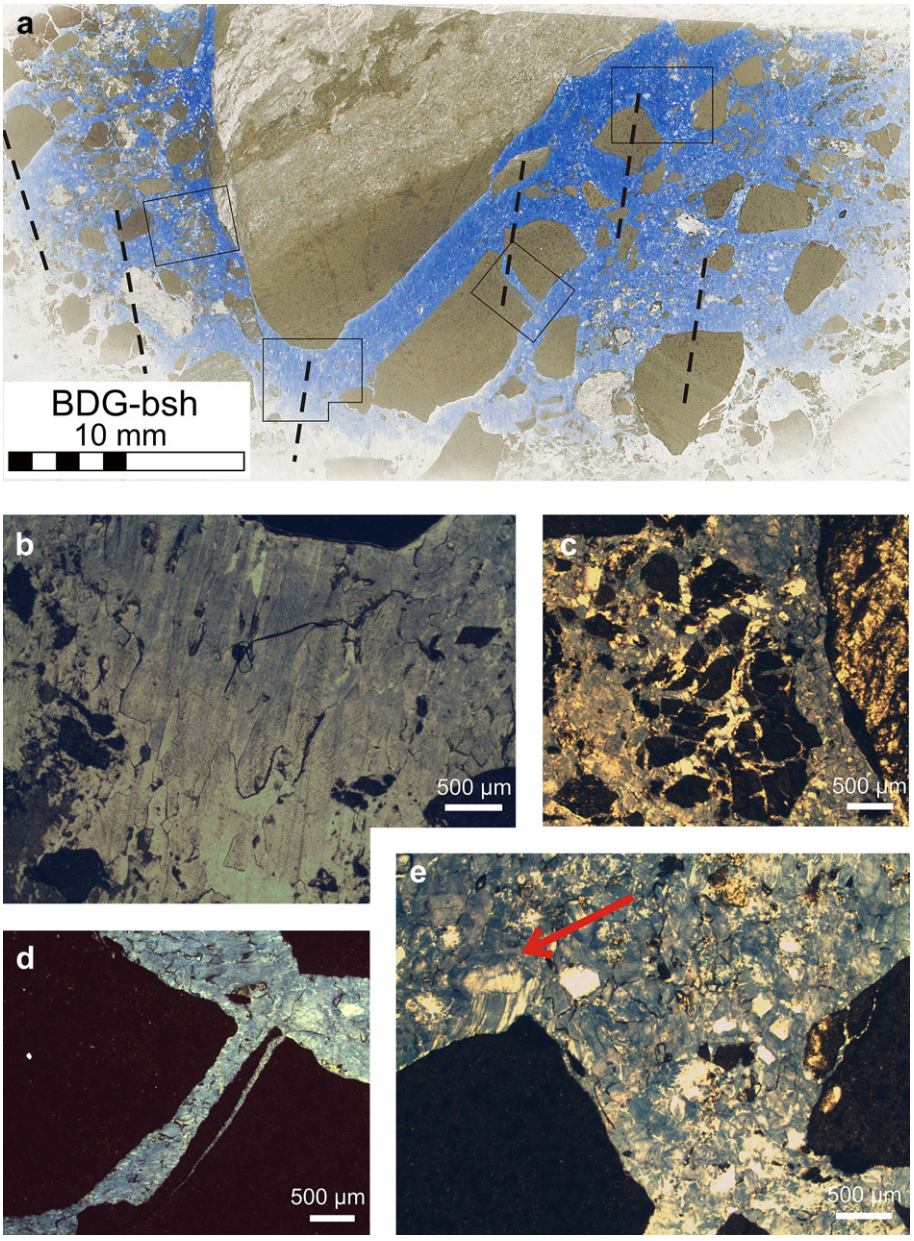

Fig. 7. (a) Irradiated thin section of sample BDG-bsh (haselgebirge, type 1). Dotted lines mark direction of mineral lineation in the rocksalt matrix. (b) Fibrous region with elongated halite crystals. (c) "Bursted mudrock", destruction in several steps, indicated by differently coloured halite. (d) Fractured mudrock with fibrous growth of halite. (e) Blocky region with equigranular grains. Note the grain, where the seam exposes partly an internally fibrous structure. The old shape fits perfectly to the piece of mudrock, indicating material support at the mudrock.

structures from sedimentation, diagenesis or early tectonic destruction. Strain shadows, filled with halite, occur locally at all scales. The appearance of colour and structure of the salt rock often changes along the galleries within a few meters (compare Schauberger, 1931, 1949, 1953, 1986; Spötl, 1989a).

Rocksalt is usually internally stretched, folded and thinned, with a mylonitic foliation. The lineation of shape-preferred halite grains and aligned particles of mudrock, anhydrite and polyhalite have the same preferred orientation. Locally, this orientation often follows the shape of incorporated rigid blocks. S-tectonites are common, with platy halite grains. Sense of shear indicators, are rare. L-tectonites were also observed in distinct shear zones with lineation of stretched coloured rocksalt. The distinguishable layers are reduced to centimeter-scale (Liniensalz in German). Most folds in rocksalt are isoclinal in a scale of meters.

Bodies of pure rocksalt within haselgebirge show characteristic features. Their outer shape is typical with concave rounding towards the centre, exposing elongated corners (Fig. 6). Black laminae of finely distributed clay suggest that salt moved from these into the surrounding rock. Halite crystallized within the surrounding haselgebirge in veins. Large rocksalt bodies contain structures like traceable foliation by red to dark-coloured banding and isoclinal folds (Fig. 6b).

5.3. Thin section analysis: haselgebirge (type 1, sample BDG-bsh)

The thin section contains halite, mudrock clasts and minor quantities of quartz, anhydrite, opaque minerals and polyhalite. The halite content is about 55 wt %, with a matrix-supported

Table 3
Characteristic microfabrics elements in thin section samples of haselgebirge from Berchtesgaden-Dürrnberg. They are characterized by fibrous halite. "x" means present, "-" means absent, parenthesis for ambiguousness. SPO = shape preferred orientation, SGR = subgrain rotation recrystallization, GBM = grain boundary migration. Old grains expose strain features like subgrains or growth rims, new grains are free of subgrains; Yellow lines/swarm bubbles are healed or tightly closed cracks, which are supposed to mark the latest stress. A = anhydrite, C = clay, G = gypsum, O = opaque, P = polyhalite, Q = quartz.

	DÜ-4C	BDG-mbsh	BDG-gh	BDG-ggrwh	BDG-bh	BDG-bsh
SPO	x	x	x	x	x	x
Grain size Ø	0.3 mm	0.5 mm	0.5 mm	0.7 mm	0.5 mm	0.4 mm
Maximum grain size	1.5 mm	1.1 mm	1.2 mm	1.4 mm	1.0 mm	1.4 mm
Chevrons	–	–	–	–	–	–
Slip lines	x	x	–	–	–	–
Old grains	(-)	(x)	x	–	–	x
SGR	(-)	x	x	x	x	x
GBM	x	x	x	x	x	x
New grains	–	–	–	–	–	x
Light-yellow grain boundaries	–	x	x	x	–	–
Core-rim by GBM	–	–	–	x	–	x
Core-rim by SGR	–	–	–	–	–	–
Fibres	x	x	x	x	x	x
Yellow lines/ swarm bubbles	–	–	x	–	–	–
Non-halite minerals	C, P, A	C, A, P, O?	C, Q, A, O, P	C, A, O, G	C, A	C, Q, A, O, P
Special features				strain shadows of gypsum		

microstructure. The average grain size of halite is 0.3 mm and ranges from 0.2 to 0.5 mm.

There are two types of rocksalt microstructures in haselgebirge. The regions of the block-shaped halite grains show lobate grain boundaries with substructure-free grains growing over grains with subgrains. Grains sometimes show a gamma irradiation-decorated blue core with a rim around it (red arrow, Fig. 7e). The colour of grains is dark to light blue or purple and they show growth zones. Slip bands are absent in the thin section.

A foliation defined by shape-preferred orientation of halite grains is seen between pieces of mudrock (Fig. 7a–e, Table 3). In fibrous regions, fibres of halite can reach 1.3 mm in length. The fibres have no subgrains (Fig. 7b). The halite forms veins between fractured pieces of mudrock, often forming a clear antitaxial seam (Fig. 7c–d, Fig. 9c–d). The size of mudrock can be several millimetres, decreasing to silt.

Intact mudrock exposes layers enriched with anhydrite. Anhydrite occurs as subhedral single grains (up to 0.6 mm in diameter), sometimes together with euhedral quartz (grain size 0.05 mm). The anhydrite exposes round solution structures. Polyhalite was found locally in this sample.

Broken and reworked mudrock clasts form lens-like clusters with internal high fitting. They form a typical microstructure of haselgebirge in thin section. As found in the other haselgebirge samples, the average size of the clusters is below 1 cm, their aspect ratio is around 1:2 (Fig. 9).

5.4. Thin section analysis: rocksalt (type 2, sample BDG-10)

The sample is almost pure rocksalt (98 wt %, Fig. 8). It was taken from a recently excavated cavern below the level Erste Tiefbausohle. The average halite grain size is 1.2 mm with occasional large grains of up to 6 mm in diameter. The microstructure is dominated by shape-preferred orientation (SPO). The grains contain subgrains. Some of the grains show evidence for grain boundary migration (GBM; Fig. 8b) and occasionally euhedral grain growth (e.g. Fig. 8c). Subgrains occur mostly within core-mantle structures along grain boundaries, giving the rock a fringed appearance (Fig. 8a). A second type of subgrains exists in the form of dark blue-coloured subgrain structures. These structures occur within the grain centres, in part overlapping the core-rim subgrain type (Fig. 8d–e).

As an accessory mineral, the rock contains anhydrite. The small euhedral grains – 0.2 mm in size – are isolated within halite grains. Clusters of these anhydrite grains give the rock a grey colour.

5.5. Thin section analysis: Berchtesgaden, Dürrnberg and Altaussee (rocksalt samples)

The rocksalt samples from Dürrnberg-Berchtesgaden and Altaussee were used for paleo flow stress estimations (piezometry). In both deposits subgrain rotation recrystallization (SGR) and GBM is common (e.g. Fig. 10c–d).

In rocksalt of Dürrnberg-Berchtesgaden, halite matrix grains are ca. 1.0 mm in size (Table 4). Isolated large grains form a visible SPO (2–10 mm). All gamma-irradiated samples from Dürrnberg-Berchtesgaden expose light-yellow grain boundaries and a core-mantle structure of subgrains. In samples from Altaussee this feature is absent (Figs. 8 and 10). Two thin sections from Berchtesgaden-Dürrnberg are special: In sample DÜ-24A, grains are nearly equigranular, 0.8 mm in size, with a polygonal microstructure and no SPO. Slip planes exist in abundance. Subgrain structures are only subordinate. Sample DÜ-30 exposes euhedral, quadratic halite grains with visible growth rims (Fig. 8c).

In the rocksalt of Altaussee, the average grain size of halite is ca. 2.0 mm, with large grains of around 10–20 mm (Table 4; e.g. Fig. 10a). Occasionally mudrock was observed inside large single halite crystals (Fig. 10b). In sample ALT-30, slip bands clearly cross the core to rim border, which makes them younger than the growth of the rim. All samples from Altaussee show slip planes (Table 4). Fibrous halite developed only around xenolithic components.

In both deposits, euhedral polyhalite crystals occur as single prismatic-shaped grains or as cloudy-red aggregates. Yellow-coloured lines with fluid inclusions and yellow or colourless swarm bubbles exist in various amounts. They cross grain boundaries, thus postdating them.

5.6. Stress-piezometry, temperature-piezometry and strain rate

The differential stress was calculated using a temperature-independent piezometer, Eq. (1). The differential stress values range between 2.0 MPa and 5.4 MPa, with an average of 2.4 ± 0.1 MPa in Altaussee and 4.6 ± 0.1 MPa in Berchtesgaden (error law of Gauss, Table 5).

We estimated the paleo-temperature in Alpine salt deposits. Differential stress, grain size and temperature relate to each other in a characteristic way (e.g. Passchier and Trouw, 2005). Ter Heege used results from triaxial deformation experiments on synthetic rocksalt with confining pressures of around 50 MPa and strain rates at 5×10^{-7} s^{-1} and faster for calibrating a temperature-dependent

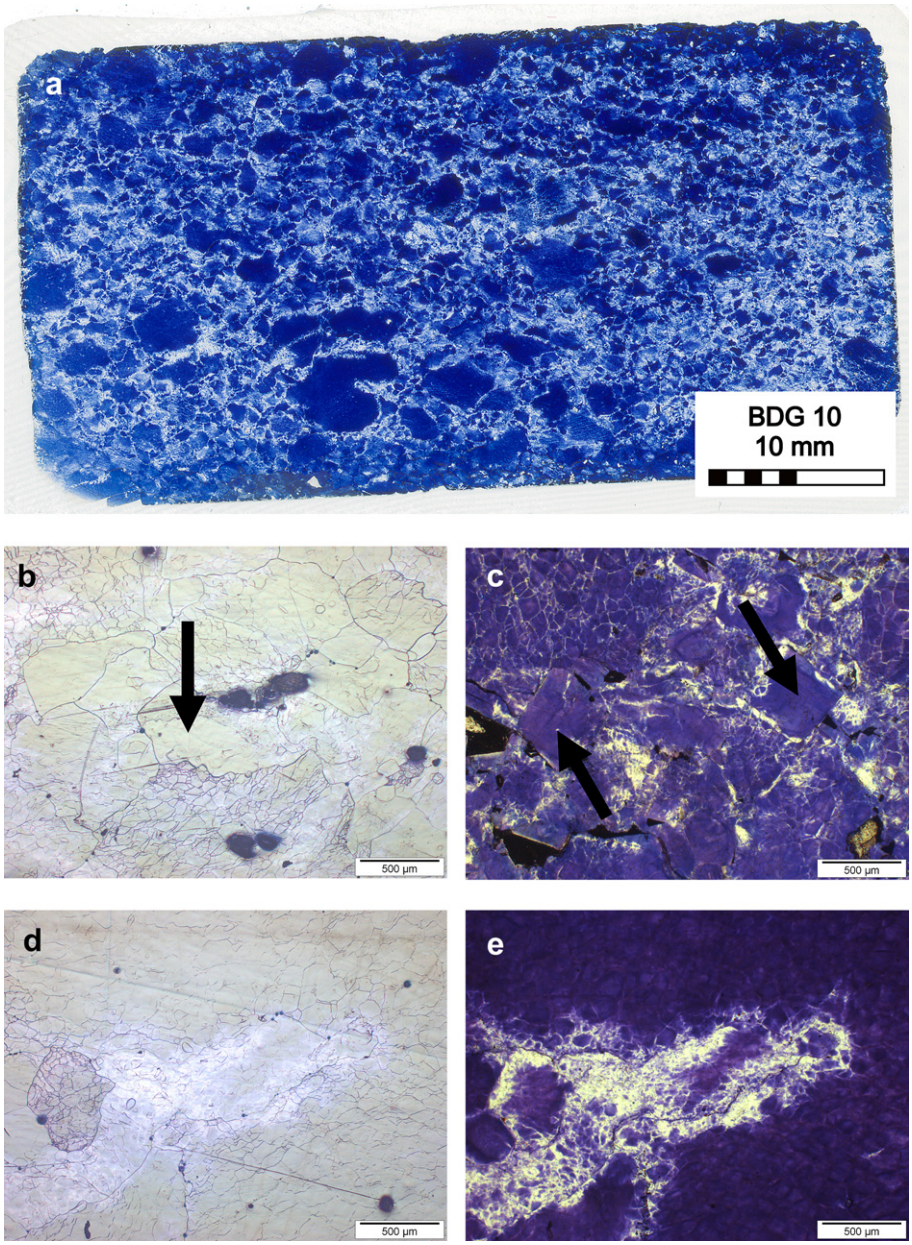

Fig. 8. (a) Irradiated thin section of sample BDG-10 with white grain boundaries (rocksalt type 2). (b) Reflected-light image: interacting GBM and SGR, arrow shows subgrain-free part consuming subgrain-rich neighbouring grain. Black dots are artefacts from preparation. (c) Sample DÜ-30 with many subgrains and subgrain-free young euhedral halite grains. (d, e) Detail of BDG-10, reflected-light image and transmitted-light image of irradiated thin section. The new grain on the left side suffered SGR already itself. The light-yellow subgrain borders exist primarily at the grain boundaries. (For interpretation of the references to colour in this figure legend, the reader is referred to the web version of this article).

grain size piezometer (Ter Heege et al., 2005). Because we observed similar microstructures in Alpine rocksalt, which shows that the same deformation mechanisms were active, GBM and SGR, we extrapolated the prediction of rocksalt behaviour to higher differential stresses and grain sizes in Fig. 11.

The average grain size of Alpine deposits is small compared to other salt deposits, for instance the Zechstein salt in Klodawa, Poland (5–20 mm, e.g Schléder, 2006). The grain size data is based on samples from field investigations, whereby only selected ones were used for thin section analysis. Halite grain size in Berchtesgaden is in the range of 0.8–1.2 mm in portions with no impurities along grain boundaries. Samples from Altaussee exhibit slightly larger grain sizes, around 1.5–2.5 mm. The upper and lower boundaries for grain size under the microscope were seen as equal to standard deviation and from this a 95% confidence was calculated (Table 6). The ratio grain size/stress is similar for Berchtesgaden-Dürrnberg and Altaussee and allows an estimation of paleo-temperatures: Altaussee 150 ± 20 °C and Berchtesgaden 110 ± 10 °C (Fig. 11).

In equation, Eq. (2), we used median values for A, Q and n, from Schoenherr et al. (2007b; Table 7). The Institut für Gebirgsmechanik GmbH, Leipzig (Ifg) carried out several triaxial tests on Alpine rocksalt, respectively from Berchtesgaden and Altaussee (Ifg, 2002, 2003, 2004, 2007). For the purpose of comparison they were done all under the same strain rate of $\dot{\varepsilon} = 1 \times 10^{-5}$ s^{-1} at room temperature. Confining pressure did not exceed 10 MPa, the differential stress was around $\Delta\sigma = 50$ MPa. The results indicate that the Alpine rocksalt has properties comparable to an "average" rocksalt (Table 7).

The range of possible temperatures – 130–170 °C for Altaussee and 100–120 °C for Berchtesgaden – reveal a range of possible strain rates: 5.7×10^{-10} to 1.8×10^{-9} s^{-1} for Altaussee and

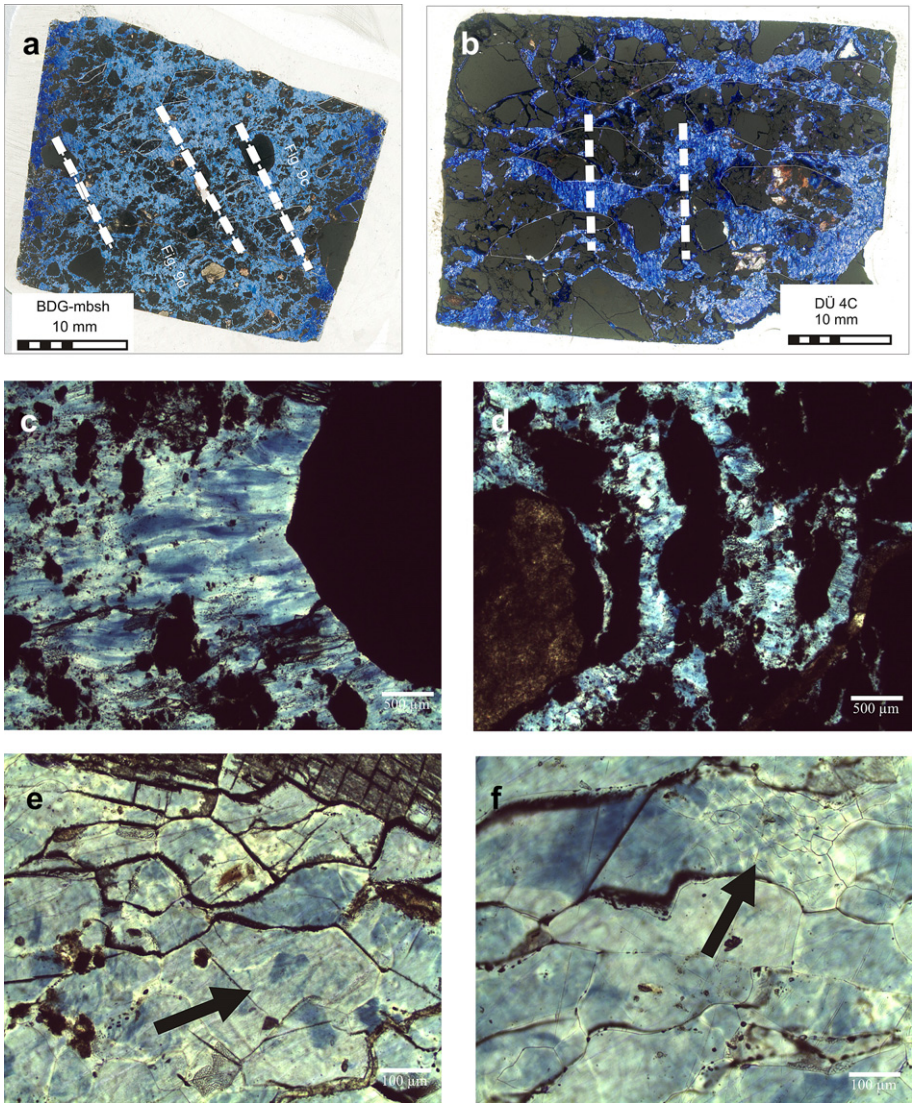

Fig. 9. (a, b) Characteristic irradiated haselgebirge samples BDG-mbsh and DÜ-4C, which differ in halite content and fitting. Lens-like clusters of broken mudrock are orientated rectangular to the halite mineral lineation. (c, d) Details of Fig. 9a: fibres in strain shadow, accumulation of halite around chipped off pieces of mudrock. (e, f) Details of BDG-mbsh: subgrain-free halite matrix grains; arrows point to growth stages and rare subgrain recrystallisation, grain boundary cracks from preparation.

3.0×10^{-9} to 5.0×10^{-9} s^{-1} for Berchtesgaden. For Altaussee, with a mean temperature of 150 °C, the strain rate is estimated to be 1.0×10^{-9} and for Berchtesgaden, with a mean temperature of 110 °C, the strain rate is estimated to be 3.8×10^{-9} (Table 8).

6. Discussion

Our observations contribute to new interpretations of the Alpine evaporites. The main results are: (1) All rock types studied are fault rocks. (2) By use of a temperature-independent subgrain size piezometer of halite mylonites, the paleo-differential stress of halite was calculated to be ca. 2.5 MPa in Altaussee and ca. 4.5 MPa in Berchtesgaden and high strain rates compared to other rocksalt types can be deduced (see below).

6.1. Structures of haselgebirge, deformation mechanisms of mudrock

In our interpretation, haselgebirge is a protocataclasite, which originated by the interaction of recrystallisation of halite and the (hydro)fracturing of mudrock under tectonic deformation. Generally, rocksalt acts as a perfect seal for fluids (e.g. hydrocarbons) due to its low permeability and the near-isotropic stress state in rocksalt bodies provides resistance to hydrofracturing of rocksalt (Peach and Spiers, 1996; Lux, 2005; Nollet et al., 2005; Schoenherr et al., 2007a). During brecciation of mudrock, we infer that water played a key role as a provider of pore pressure and transport agent. A possible source for the hydrous fluid is mudrock or gypsum dehydration (Borchert and Muir, 1964; Tucker, 1991). Mudrock may have hydrofractured into a crush breccia under very low effective stress.

In halite, both recovery processes are present, subgrain rotation recrystallization (SGR) and grain boundary migration (GBM). Growth banding (types 1, 2), and the development of fibres (mainly in haselgebirge, microstructural type 1) indicate solution–precipitation processes. We observed that halite accumulates around mudrock components, which results in a matrix-supported structure. Halite fibres crystallize at the contact to the mudrock (Fig. 9c). The occurrence of such fibres points to precipitation from a hydrous fluid during opening of a fracture (Schléder and Urai, 2007), documenting the migration of halite into haselgebirge (compare Fig. 6b). During cataclastic flow, the clasts form lens-like clusters perpendicular to the transport direction and parallel to the plain strain direction, which is marked by the SPO of the halite

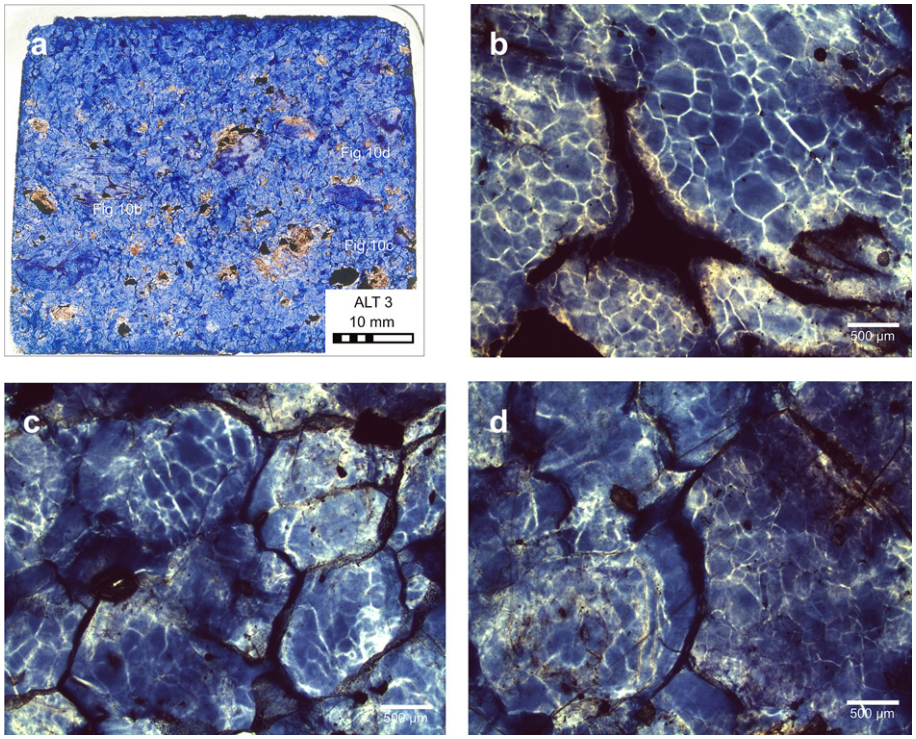

Fig. 10. (a) Overview micrograph of gamma-irradiated sample ALT-3. Note large, old halite grains with SPO, flakes are polyhalite and mudrock. (b) The large halite grains include mudrock with bizarre shapes, which formed intergranular between former halite grains. (c) Interacting GBM and SGR: microstructure of polygonal, equigranular matrix. Grain boundaries appear as dark lines, the subgrains as white polygonal lines. (d) Detailed view of a lobate-shaped grain boundary, which bulge into the subgrain-rich old grain.

Table 4
Microfabrics recognized in thin section of rocksalt samples from Dürrnberg-Berchtesgaden and Altaussee. The salt bodies differ in grain size. Altaussee halite is characterised by slip lines, Dürrnberg-Berchtesgaden by SGR and light-yellow grain boundaries. B = bloedite, further abbreviations and explanations as in Table 3.

	ALT-3	ALT-26	ALT-30	ALT-37A	ALT-39	DÜ-7C	DÜ-24A	DÜ-30	DÜ-41D	BDG-10
SPO	2x	x	2x	x	x	x	(-)	x	x	x
Grain size Ø	1.5 mm	1.5 mm	2.0 mm	2.5 mm	2.5 mm	0.7 mm	0.8 mm	1.1 mm	1.0 mm	1.2 mm
Maximum grain size	12.0 mm	7.5 mm	5.0 mm	16.0 mm	10.0 mm	6.0 mm	1.8 mm	2.5 mm	6.0 mm	6.0 mm
Chevrons	–	–	–	–	–	–	–	–	–	–
Slip lines	x	x	x	x	x, crossed	(-)	x, crossed	–	(-)	–
Old grains	x	x	x	x	x	x	(-)	(x)	(x)	x
SGR	x	x	x	x	x	x	x	x	x	x
GBM	x	x	x	x	x	x	x	x	x	x
New grains	–		(-)	–	(x)	–	–	x	–	–
Light-yellow grain boundaries	–	x	–	–	x	x	x	x	x	x
Core-rim by GBM	–	x	x	–	x	–	–	–	–	–
Core-rim by SGR	–	–	–	–	–	(x)	–	x	x	x
Fibres	x	x	–	–	x	–	–	x	–	–
Yellow lines/ swarm bubbles	–	x	x	x	x	x	x	–	x	–
Non-halite minerals	C, P, A	C, P	C, P, A	C, P	C, P, A	C, P, A, B	C, P, A	C, P, A	C, P	A
Special features							Polygonal appearance, blue subgrain borders	Euhedral new grains, intergranular mudrock		Blue subgrain borders

Table 5
Calculated differential stress. The estimate of subgrain size and calulation of differential stress was made as described in Schléder and Urai (2005).

Sample	Grain size diameter [µm]	Number of subgrains	Subgrain size diameter [µm]	Subgrain size standard dev. [µm]	Mean Δσ (95% confidence) [MPa]	Δσ [MPa]	Mean value [MPa]
ALT-3	1571	168	99	70	1.8–2.2	2.0 ± 0.2	ALT: 2.4 ± 0.1
ALT-37A	1439	259	71	55	2.4–2.9	2.6 ± 0.2	
ALT-26	1455	309	69	46	2.5–2.9	2.7 ± 0.2	
ALT-gh	603	121	44	33	3.6–4.5	4.0 ± 0.5	–
BDG-10	781	328	36	24	4.5–5.1	4.7 ± 0.2	BDG: 4.6 ± 0.1
BDG-13	535	218	31	19	5.2–5.6	5.4 ± 0.2	
BDG-19A	1657	390	66	52	2.6–3.0	2.8 ± 0.2	
DÜ-41	600	267	31	20	5.1–5.8	5.4 ± 0.3	

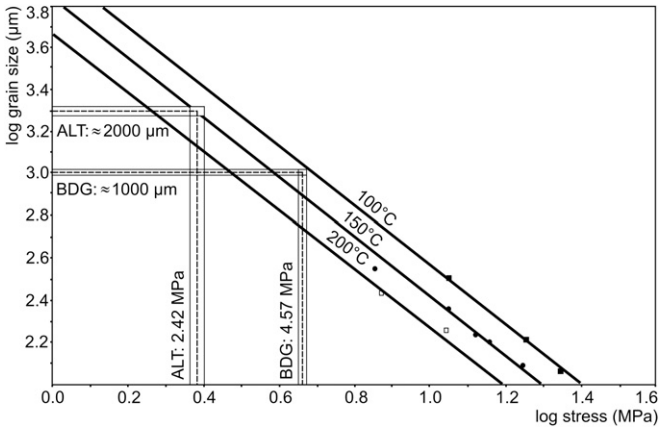

Fig. 11. Diagram modified after Ter Heege et al. (2005) showing the relation between grain size and differential stress and temperature. Temperatures reached in Altaussee and Berchtesgaden are in the same range.

Schléder and Urai, 2007). Considering the high temperatures and stresses, the strain rate of the rocksalt studied is of the highest natural strain rate inferred in rocksalt so far: 10^{-10}–10^{-9} s^{-1}.

Schléder and Urai (2007) observed protomylonites and distinct layers of mylonites in salt glaciers in Iran. The protomylonites show well-developed subgrains, suggesting deformation mainly by dislocation creep processes, similar to Alpine rocksalt. Very fine grained mylonites, showing only oriented fibrous overgrowths and growth banding, suggesting only solution-precipitation creep and grain boundary sliding, are missing in Alpine rocksalt. But fine-grain size, fibres and growth banding, indicating solution-precipitation creep, are seen in haselgebirge.

In haselgebirge, the higher the halite content, the more grains with subgrains developed pointing to deformation of halite by subgrain rotation reccrystallization. However, the absence of plastic crystal deformation in the fibrous halite between the mudrock clasts is puzzling, especially considering the subgrains and evidence for dislocation creep in the more halite-rich parts of the

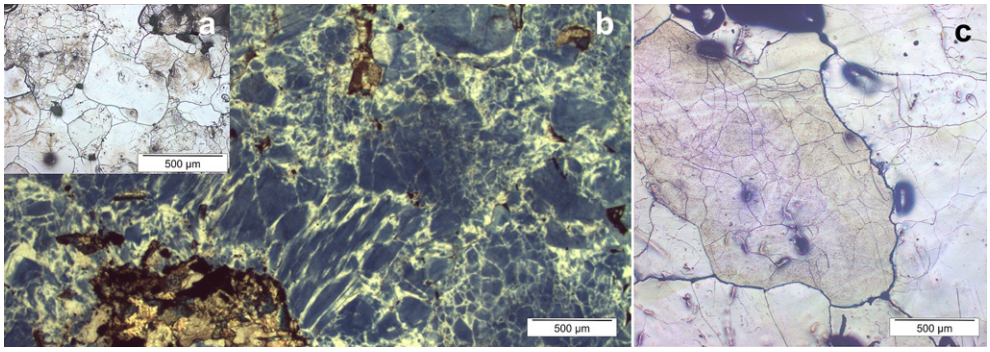

Fig. 12. Halite subgrains under the same magnification. (a) Sample DÜ-41 exposes the highest measured value of 5.4 MPa (b) DÜ-30; note also halite fibres, which developed at xenoliths within the rocksalt matrix (c) The differential stress of ALT-3 is 2.0 MPa, which is a range typical for diapirs, for instance in Permian Zechstein Salt (Schléder, 2006) or in Oman Infra-Cambrian Ara Salt (Schoenherr, 2008).

grains (Fig. 9a, b). The clasts can develop a polished dark skin. Furthermore, such mudrock clasts are found entirely isolated within the salt matrix (e.g. Fig. 5a).

The average subgrain size diameter of slightly deformed rocksalt from Hengelo, Netherlands is ca. 300–400 µm (Schleder and Urai, 2005). The average subgrain size diameter of our samples from Berchtesgaden-Dürrnberg is much smaller, ca. 30–40 µm (Fig. 12). In comparison, synthetic rocksalt in triaxial tests has subgrain sizes of 10–15 µm (Trimby et al., 2000b; Peach et al., 2001; Watanabe and Peach, 2002; Ter Heege et al., 2005; Fig. 13). The deduced temperatures and the deduced strain rates of our samples studied are different from other rocksalt types: salt diapir rise 10^{-16}–10^{-11} s^{-1}, salt glacier 10^{-11}–10^{-9} s^{-1} (Jackson et al., 1994;

Table 6
Mean values with error estimates of grain size from thin section.

Sample	Grain size (95% confidence)	Grain size [mm]	Mean value [mm]
ALT-3	1.3-1.7	1.5 ± 0.2	ALT: 2.0 ± 0.1
ALT-26	1.4-1.6	1.5 ± 0.1	
ALT-30	1.8-2.2	2.0 ± 0.2	
ALT-37A	2.3-2.7	2.5 ± 0.2	
ALT-39	2.4-2.6	2.5 ± 0.1	
DÜ-7C	0.6-0.8	0.7 ± 0.1	DÜ/BDG: 1.0 ± 0.1
DÜ-24A	0.7-0.9	0.8 ± 0.1	
DÜ-30	0.9-1.3	1.1 ± 0.2	
DÜ-41D	0.9-1.1	1.0 ± 0.1	
BDG-10	1.1-1.3	1.2 ± 0.1	

same rock. There are two possible hypotheses to explain this: (i) there were two phases of deformation; one at high stress leading to plastic crystal deformation of the halite, followed by a phase at much lower stress during which the fibrous halite recrystallized or precipitated; (ii) during one phase of deformation, the parts of the rock in which the mudrock clasts formed a load-supporting frame, stresses were mostly carried by the mudrock clasts and the fibrous halite could precipitate between the clasts at very low stress, without plastic crystal deformation.

Hypothesis (i) is unlikely considering the location of the fibres exclusively between the mudrock clasts. If recrystallization was the operating process, one would expect fibrous recrystallized halite in more halite-rich parts of the rock and this is not the case. Also no halite veins exist in the halite-rich parts of the rock. Therefore we favour hypothesis (ii). In this model it is interesting to note that the antitaxial fibres point to a long series of crack-seal events at the halite–mudrock interface, without the formation of open fractures,

Table 7
Material parameters A, Q, n from 10 rocksalt deposits (Schoenherr et al., 2007b).

Salt rock	A (MPa^{-n} s^{-1})	Q (J mol^{-1})	n (−)
Maximum	7.8×10^{-3}	74530	5.3
Minimum	1.8×10^{-9}	32400	3.4
Mean value	1.0×10^{-3}	56747	4.7
Median	5.6×10^{-5}	54380	5.0

Table 8
Calculated strain rates from Altaussee and Berchtesgaden-Dürrnberg.

Formula $[\varepsilon'] = s^{-1}$	Altaussee 130–170 °C (mean 150 °C)	Berchtesgaden-Dürrnberg 100–120 °C (mean 110 °C)
$\varepsilon'_{PS} + \varepsilon'_{DC}$	5.7×10^{-10} (min. 130 °C)	3.0×10^{-9} (min. 100 °C)
$\varepsilon'_{PS} + \varepsilon'_{DC}$	1.8×10^{-9} (max. 170 °C)	5.0×10^{-9} (max. 120 °C)
$\varepsilon'_{\text{pressure solution}}$	3.1×10^{-10} (mean 150 °C)	2.5×10^{-9} (mean 110 °C)
$\varepsilon'_{\text{dislocation creep}}$	7.0×10^{-10} (mean 150 °C)	1.3×10^{-9} (mean 110 °C)
ε' compound $(=\varepsilon'_{PS} + \varepsilon'_{DC})$	1.0×10^{-9} (mean 150 °C)	3.8×10^{-9} (mean 110 °C)
ε' unified, median for *A*, *Q*, *n*	8.6×10^{-10} (mean 150 °C)	4.0×10^{-9} (mean 110 °C)

Figs. 1 and 2). The accurate age of tectonic deformation within the haselgebirge is not well constrained and may include several stages between the Late Jurassic and Neogene. Many of the old anhydrite and polyhalite structures were preserved (e.g. veins with fibrous polyhalite, folded anhydrite). When small euhedral anhydrite and prismatic polyhalite crystals were completely overgrown and incorporated into the halite, fluids migrated through the salt body. In the Late Jurassic, at 145–154 Ma, the growth of feldspar documents the movement of hot brines within the Haselgebirge unit (Spötl et al., 1998a, 1998b). In the middle Early Cretaceous, at 125 Ma, fluorite precipitated from saline waters forming veins

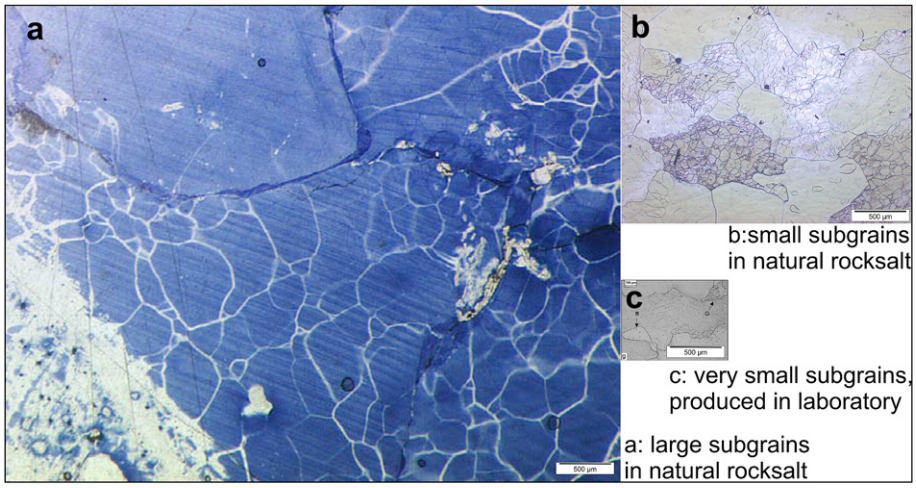

Fig. 13. Halite subgrains under the same magnification. (a) Schléder and Urai (2005), Hengelo, salt layer A, calculated flow strain: ca. 0.70 MPa, deformation rate around ca. 10^{-13}–10^{-14} s^{-1}. (b) This study, sample BDG 10, calculated flow strain 4.73 MPa, deformation rate around ca. 10^{-9}–10^{-10} s^{-1} (c) Ter Heege et al. (2005), sample 11RS200, flow strain 11.1 MPa, deformation rate 2.4×10^{-5} s^{-1}.

providing interesting constraints on the conditions of deformation of the surrounding more connected halite.

6.2. The Haselgebirge Formation

In halite, we did not find parallel bands or chevrons-like patterns of fluid inclusions. Such arrangements are interpreted as primary diurnal crystal growth structures and common in sedimentary salt rocks (e.g. Roedder, 1984). Therefore, halite must have recrystallized more or less completely.

Based on a variety of geothermometers, the Haselgebirge Formation reached temperatures of 180 °C in Hallstatt (Spötl and Hasenhüttl, 1998) and even more than 250 °C in Bad Ischl, Altaussee (Wiesheu and Grundmann, 1994) and Berchtesgaden (Kralik et al., 1987). Similar temperatures were found in gypsum/anhydrite deposits of central NCA. One of the most reliable temperature measurements was conducted with fluid inclusions in quartz, which revealed 220–260 °C (Spötl et al., 1998b). The Alpine mudrock consists mainly of illite/muscovite, chlorite and mixed-layered clays (Glück, in press). In the mine of Hall in Tyrol, mixed-layered clays contain less than 5% smectite (Spötl, 1992). This is further evidence that temperatures necessary for maximum water expulsion were reached – at least once in the history of the mudrock. At a temperature >100 °C, when fluid was present and mobile, we speculate the starting point for (further) halokinesis and detachement of the Juvavic units from their basement and the onset of intense mudrock fracturing (compare Lewis and Holness, 1996).

The main nappe stacking started at the beginning of Late Jurassic and lasted to the Middle Cretaceous (e.g. Mandl, 2000; within limestones and dolomites of the overlying Middle Triassic Gutenstein Formation (Götzinger and Grum, 1992). In the Middle Cretaceous at ca. 90–97 Ma, a second stage of feldspar growth followed (Spötl et al., 1998a).

Our temperature estimates (≈150 °C, ≈110 °C) are slightly different than reported peak temperatures in the literature (≥200 °C). The temperature during the formation of the observed microfabrics in rocksalt, therefore, was already lower than the peak temperatures. The deduced strain rates are very high, e.g. a 100 m salt sheet would creep 3 m/a. Possibly, the fast deformation occurred at short time intervals only, in connection with earthquakes. Trepmann and Stöckert (2003) discuss synseismic loading with postseismic creep in the plastosphere (underlying the schizosphere, where earthquakes nucleate). They found evidence for rapid deformation in quartz crystals (glide-controlled deformation laminae and healed microcracks) and instantaneous succession of stress reduction by dislocation creep with subgrain rotation recrystallization. They deduced deformation rates of 10^{-11}–10^{-10} s^{-1}.

7. Conclusions

- Haselgebirge is mostly a protocataclasite, whereas kerngebirge and pure rocksalt are mostly mylonites and ultramylonites.
- No primary features like linear arrangements of fluid inclusions, chevrons or parallel lines were identified in Alpine salt samples. Halite, therefore, recrystallized more or less completely.
- The flow stress is the highest measured so far in rocksalt, deduced from a temperature-independent subgrain piezometer. The

estimated mean temperatures are 150 ± 20 °C in Altaussee and 110 ± 10 °C in Berchesgaden.
- The estimated deformation rate is about 10^{-10}–10^{-9} s^{-1}.
- Mudrock was fractured under deviatoric stress and high fluid pressure. The mudrock disintegrated to the present-day haselgebirge with clast-size between micrometers to ca. 10 cm.

Acknowledgements

We acknowledge detailed and constructive reviews by Christoph Spötl, Gernold Zulauf and Thomas Blenkinsop. Isabella Merschdorf proofread the final manuscript. The final work was supported by grant P22728 of the Austrian Research Agency (FWF). We thank the mining companies Südsalz GmbH, Berchtesgaden salt mine and Salinen Austria AG for their support in access to the underground sites and test data. Stefan Kellerbauer is thanked for his help in organizing, discussions and personal advice.

References

Alavi, M., 2007. Structures of the Zagros fold-thrust belt in Iran. American Journal of Science 307, 1064–1095.
Armann, M., 2008. Microstructural and Textural Developement in Synthetic Rocksalt Deformed in Torsion. Dissertation No. 17663. University ETH Zürich.
Arnberger, K., 2006. Detachement Folding above the Permian Haselgebige: Palinspastic Reconstruction of Alpine West-directed Thrusting (Plassen, Hallstatt, Upper Austria). Diploma thesis. University of Vienna.
Borchert, H., Muir, R.O., 1964. The Origin, Metamorphism and Deformation of Evaporites. In: Salt Deposits. Van Nostrand, London, New York, Toronto.
Braun, R., 1998. Die Geologie des Hohen Gölls. National Park Berchtesgaden Forschungsbericht 40.
Buch, L.v., 1802. Geognostische Beobachtungen auf Reisen durch Deutschland und Italien. Band 1. Haude und Spencer, Berlin.
Carter, N.L., Handin, J., Russell, J.E., Horseman, S.T., 1993. Rheology of rocksalt. Journal of Structural Geology 15, 1257–1271.
Charpentier, D., Worden, R.H., Dillon, C.G., Aplin, A.C., 2003. Fabric developement and the smectite to illite transition in Gulf of Mexico mudstones: an image analysis approach. Journal of Geochemical Exploration 78–79, 459–463.
Couzens-Schultz, B.A., Wiltschko, D.V., 2000. The control of the smectite-illite transition on passive-roof duplex formation: Canadian Rockies Foothills, Alberta. Journal of Structural Geology 22, 207–230.
Dallmeyer, R.D., Neubauer, F., Fritz, H., 2008. The Meliata Suture in the Carpathians: Regional Significance and Implications for the Evolution of High-pressure Wedges within Collisional Orogens. In: Siegesmund, S., Fügenschuh, B., Froitzheim, N. (Eds.), Tectonic Aspects of the Alpine-Dinaride-Carpathian System. Geological Society Special Publications, London, vol. 298, pp. 101–115.
Davis, D.M., Engelder, T., 1985. The role of salt in Fold-and-Thrust Belts. Tectonophysics 119, 67–88.
de Meer, S., Spiers, C.J., Nakashima, S., 2005. Structure and diffusive properties of fluid-filled grain boundaries: an in-situ study using infrared (micro) spectroscopy. Earth and Planetary Science Letters 232, 403–414.
Deng, X., Sun, Y., Lei, X., Lu, Q., 1996. Illite/Smectite diagenesis in the NanXiang, Yitong, and north China Pemian – Carboniferous basins: application to Petroleum exploration in China. AAPG Bulletin 80 (2), 157–173.
Deutsches Institut für Normung e.V., 2004. DIN EN ISO 14688-2: Geotechnische Erkundung und Untersuchung – Benennung, Beschreibung und Klassifizierung von Boden; Teil 2: Grundlagen für Bodenklassifizierungen. Beuth, Berlin, Wien, Zürich.
Faupl, P., Wagreich, M., 2000. Late Jurassic to Eocene Paleogeography and Geodynamic evolution of the eastern Alps. In: Neubauer, F., Höck, V. (Eds.), Aspects of Geology in Austria. Mitteilungen der Österreichischen Geologischen Gesellschaft, 92, pp. 79–94.
Frank, W., Schlager, W., 2006. Jurassic strike slip versus subduction in the Eastern Alps. International Journal of Earth Sciences 95, 431–450.
Gawlick, H.-J., Höpfer, N., 1996. Die mittel- bis frühjurassische Hochdruckmetamorphose der Hallstätter Kalke (Trias) der Pailwand – ein Schlüssel zum Verständnis der frühen Geschichte der Nördlichen Kalkalpen. In: Thein, J., Schäfer, A. (Eds.), Geologische Stoffkreisläufe und ihre Veränderungen durch den Menschen. Schriftenreihe der Deutschen Geologischen Gesellschaft 1/1, pp. 30–32.
Gawlick, H.-J., Lein, R., 2000. Die Salzlagerstätte Hallein-Bad Dürrnberg. Exkursionsführer Sediment 2000. Mitteilungen der Gesellschaft der Geologie- und Bergbaustudenten in Österreich 44, 263–280.
Gawlick, H.-J., Schlagintweit, F., 2006. Berriasian drowning of the Plassen carbonate platform at the type-locality and its bearing on the early Eoalpine orogenic dynamics in the Northern Calcareous Alps (Austria). International Journal of Earth Sciences 95, 451–462.
Gawlick, H.-J., Krystyn, L., Lein, R., 1994. Conodont colour alteration indices: palaeotemperatures and metamorphism in the Northern Calcareous Alps – a general view. Geologische Rundschau 83, 660–664.
Glück, C., in press. Über die Tonminerale des Haselgebirges. Unpublished report, University of Salzburg, p. 26.
Götzinger, M.A., Grum, W., 1992. Die Pb-Zn-F-Mineralisationen in der Umgebung von Evaporiten der Nördlichen Kalkalpen, Österreich – Herkunft und Zusammensetzung der fluiden Phase. Mitteilungen der Gesellschaft der Geologie- und Bergbaustudenten in Österreich 38, 47–56.
Grabner, M., Klein, A., Geihofer, D., Reschreiter, H., Barth, F., Sormaz, T., Wimmer, R., 2007. Bronze age dating of timber from the salt-mine at Hallstatt, Austria. Dendrochronologia 24, 61–68.
Habermüller, M., 2005. West-directed Thrusting in the Dachstein Nappe: Quantification of the Eo-Alpine Deformation Around the Echerntal Valley (Hallstatt, Austria). Dipolma thesis. University of Vienna.
Hejl, E., Grundmann, G., 1989. Apatit-Spaltspurdaten zur thermischen Geschichte der Nördlichen Kalkalpen, der Flysch- und Molassezone. In: Jahrbuch der Geologischen Bundesanstalt132/1 191–212.
Hickman, S.H., Evans, B., 1995. Kinetics of pressure solution at halite-silica interfaces and intergranular clay films. Journal of Geophysical Research 100 (No. B7), 13,113–13,132.
Institut für Gebirgsmechanik GmbH, 2002. Ergebnisse einaxialer Druckversuche und dreiaxialer Mehrstufenversuche an Steinsalzproben aus Bohrkernen aus dem Bohrlochsondenfeld Bad Ischl der Salinen Austria AG (Unpublished report, Leipzig).
Institut für Gebirgsmechanik GmbH, 2003. Einaxiale Druckversuche und dreiaxiale Mehrstufenversuche an Steinsalzprüfkörpern aus Bohrkernen aus dem alpinen Haselgebirge des Salzbergwerkes Berchtesgaden (Unpublished report, Leipzig).
Institut für Gebirgsmechanik GmbH, 2004. Ergebnisse einaxialer Druckversuche und dreiaxialer Mehrstufenversuche an Steinsalzproben aus Bohrkernen aus dem Salzbergbau Altaussee (Unpublished report, Leipzig).
Institut für Gebirgsmechanik GmbH, 2007. Ergebnisse einaxialer Druckversuche und dreiaxialer Mehrstufenversuche an Haselgebirgsproben aus dem Salzbergbau Hallstatt (Unpublished report, Leipzig).
Jackson, M.P.A., Vendeville, B.C., Schultz-Ela, D.D., 1994. Structural dynamics of salt systems. Annual reviews. Earth and Planetary Sciences 22, 93–117.
Jadoon, I.A.K., Frisch, W., 1997. Hinterland-vergent tectonic wedge below the Riwat thrust, Himalayan foreland, Pakistan: implications for hydrocarbon exploration. AAPG Bulletin 81, 438–448.
Kellerbauer, S., 1996. Geologie und Geomechanik der Salzlagerstätte Berchtesgaden. In: Spaun, G., Miller, H., Wohnlich, S., Reihe, B. (Eds.), Münchener Geologische Hefte. Angewandte Geologie 2.
Kirchner, E., 1980. Vulkanite aus dem Permoskyth der Nördlichen Kalkalpen und ihre Metamorphose. Mitteilungen der Österreichen Geologischen Gesellschaft 71/72, 385–396.
Klein, A., 2006. Bronzezeitliche Holznutzung in Hallstatt. Diploma thesis. University of Natural Resources and Applied Life Sciences, Vienna.
Kralik, M., Krumm, H., Schramm, J.M., 1987. Low Grade and Very Low Grade Metamorphism in the Northern Calcareous Alps and in the Greywacke Zone: Illite – Crystallinity Data and Isotopic Ages. In: Flügel, H.W., Faupl, P. (Eds.), Geodynamics of the Eastern Alps. Deutike, Wien.
Lewis, S., Holness, M., 1996. Equilibrium halite-H_2O dihedral angles: high rock-salt permeability in the shallow crust? Geology 24, 431–434.
Linzer, H.-G., Ratschbacher, L., Frisch, W., 1995. Transpressional collision structures in the upper crust: the fold-thrust belt of the Northern Calcerous Alps. Tectonophysics 242, 41–61.
Lohkämper, T., Jordan, G., Röller, K., Stöckert, B., Schmahl, W., 2004. On the influence of fluids on deformation process of halite crystals. Geochemica et Cosmochimica Acta 68 (11), A173.
Lux, K.-H., 2005. Zum langfristigen Tragverhalten von verschlossenen solegefüllten Salzkavernen – ein neuer Ansatz zu physikalischer Modellierung und numerischer Simulation. Theoretische und laborative Grundlagen. Erdöl Erdgas Kohle 121 (11), 414–422.
Magara, K., 1980. Comparison of porosity-depth relationships of shale and sandstone. Journal of Petroleum Geology 3, 175–185.
Mandl, G.W., 1982. Jurassische Gleittektonik im Bereich der Hallstätter Zone zwischen Bad Ischl und Bad Aussee (Salzkammergut Österreich). Mitteilungen der Gesellschaft der Geologie- und Bergbaustudenten in Österreich 28, 55–76.
Mandl, G.W., 2000. The alpine sector of the Thetyan shelf – Example of Triassic to Jurassic sedimentation and deformation from the northern Calcerous. In: Aspects of Geology in Austria. Mitteilungen der Österreichischen Geologischen Gesellschaft, 92, pp. 61–77.
Martin, B., Röller, K., Stöckert, B., 1999. Low-stress pressure solution experiments on halite single-crystals. Tectonophysics 308, 299–310.
Mayrhofer, H., 1955. Beiträge zur Kenntnis des alpinen Salzgebirges/ mit einer strukturellen und stofflichen Bearbeitung des Ischler Salzbergs und einem Entwurf einer tektonischen Entstehungshypothese des Haselgebirges. Zeitschrift der Deutschen Geologischen Gesellschaft 105, 752–775.
Medwenitsch, W., 1958. Die Geologie der Salzlagerstätten Bad Ischl und Alt-Aussee (Salzkammergut). Mitteilungen der Geologischen Gesellschaft in Wien 50, 133–199.
Neubauer, F., Genser, J., Handler, R., 2000. The Eastern Alps: result of a two-stage collision process. In: Neubauer, F., Höck, V. (Eds.), Aspects of Geology in Austria. Mitteilungen der Österreichischen Geologischen Gesellschaft, 92, pp. 117–134.

Nollet, S., Hilgers, C., Urai, J.L., 2005. Sealing of fluid pathways in overpressure cells: a case study from the Buntsandstein in the Lower Saxony Basin (NW Germany). International Journal of Earth Sciences 94, 1039–1055.
Oberhauser, R., 1980. Der Geologische Aufbau Österreichs. Springer, Wien et al.
Passchier, C.W., Trouw, R.A.J., 2005. Microtectonics, second ed. Springer, Berlin et al.
Peach, C.J., Spiers, C.J., 1996. Influence of crystal plastic deformation on dilatancy and permeability development in synthetic salt rock. Tectonophysics 256, 101–128.
Peach, C.J., Spiers, C.J., Trimby, P.W., 2001. Effect of confining pressure on dilatation, recrystallisation, and flow of rock salt at 150°C. Journal of Geophysical Research B: Solid Earh 106 (7), 13,315–13,328.
Pichler, H., 1963. Geologische Untersuchungen im Gebiet zwischen Rossfeld und Markt Schellenberg im Berchtesgadener Land. Beihefte Zum Geologischen Jahrbuch 48, 29–204.
Plöchinger, B., 1990. Erläuterungen zu Blatt 94 Hallein. – Geologische Karte der Republik Österreich 1:50 000. Geologische Bundesanstalt, Wien.
Plöchinger, B., 1996. Das Halleiner Salinargebiet (Salzburg) im Geotopschutz-Projekt. Jahrbuch der Geologischen Bundesanstalt 139 (4), 497–504.
Popp, T., Kern, H., Schulze, O., 2001. Evolution of dilatancy and permeability in rock salt during hydrostatic compaction and triaxial deformation. Journal of Geophysical Research 106 (No. B3), 4061–4078.
Proisl, M., 2003. Planung der Aus- und Vorrichtung westlich des Zentralschachtes und unterhalb des Erbstollenhorizontes des Salzbergbaues Altaussee. Diploma thesis. Montanistic University of Leoben.
Rantitsch, G., Russegger, B., 2005. Organic maturation within the central northern Calcareous Alps (Eastern Alps). Austrian Journal of Earth Sciences 98, 68–76.
Richter, D.K., Füchtbauer, H., 1981. Merkmale und Genese von Breccien und ihre Bedeutuing im Mesozoikum von Hydra (Griechenland). Zeitschrift der deutschen geologischen Gesellschaft 132, 451–501.
Roedder, E., 1984. The fluids in salt. American Mineralogist 69, 413–439.
Saffer, D.M., Underwood, M.B., Mckiernan, A.W., 2008. Evaluation of factors controlling smectite transformation and fluid production in subduction zones: application to the Nankai Trough. Island Arc 17, 208–230.
Schauberger, O., 1931. Die Fließstrukturen im Hallstätter Salzlager. Berg- und Hüttenmännische Monatshefte 79, 27–38.
Schauberger, O., 1949. Die stratigraphische Aufgliederung des alpinen Haselgebirges. Berg- und hüttenmännische Monatshefte 94 (3), 46–56.
Schauberger, O., 1953. Zur Genese des alpinen Haselgebirges. Zeitschrift der Deutschen Geologischen Gesellschaft 105, 736–751.
Schauberger, O., 1986. Bau und Bildung der Salzlagerstätten des ostalpinen Salinars. Archiv für Lagerstättenforschung der Geologischen Bundesanstalt 7, 217–254.
Schauberger, O., Zankl, H., Kühn, R., Klaus, W., 1976. Die geologischen Ergebnisse der Salzbohrungen im Talbecken von Bad Reichenhall. Geologische Rundschau 65, 558–579.
Schenk, O., Urai, J.L., 2004. Microstructural evolution and grain boundary structure during static recrystallization in synthetic polycrystals of Sodium Chloride containing saturated brine. Contributions to Mineralogy and Petrology 146, 671–682.
Schenk, O., Urai, J.L., 2005. The migration of fluid-filled grain boundaries in recrystallizing synthetic bischofite: first results of in-situ high-pressure, high-temperature deformation experiments in transmitted light. Journal of Metamorphic Geology 23, 695–709.
Schléder, Z., 2006. Deformation Mechanisms of Naturally Deformed Rocksalt. Dissertation. University RWTH Aachen.
Schléder, Z., Urai, J.L., 2005. Microstructural evolution of deformation-modified primary halite from the Middle Triassic Röt Formation at Hengelo, The Netherlands. International Journal of Earth Sciences 94, 941–955.
Schléder, Z., Urai, J.L., 2007. Deformation and recrystallization mechanisms in mylonitic shear zones in naturally deformed extrusive Eocene–Oligocene rocksalt from Eyvanekey plateau and Garmsar hills (central Iran). Journal of Structural Geology 29, 241–255.
Schmid, S.M., Fügenschuh, B., Kissling, E., Schuster, R., 2004. Transects IV, V, VI: the Alps and their Forelands. In: Cavazza, W., Roure, F.M., Spakman, W., Stampfli, G.M., Ziegler, P.A. (Eds.), The TRANSMED Atlas. The Mediterranean Region from Crust to Mantle. Springer, Berlin.
Schmidegg, O., 1951. Die Stellung der Haller Salzlagerstätte im Bau des Karwendelgebirges. Jahrbuch der Geologischen Bundesanstalt 94, Festschrift (1949/51), pp. 159–207.
Schoenherr, J., 2008. The Evolution of Halite, Solid Bitumen and Carbonate in the Petroleum System of the South Oman Salt Basinion mechanisms of naturally deformed rocksalt. PhD Thesis, University RWTH Aachen.
Schoenherr, J., Urai, J.L., Kukla, P.A., Littke, R., Schléder, Z., Larroque, J.-M., Newall, M.J., Al-Abry, N., Al-Siyabi, H.A., Rawani, Z., 2007a. Limits to the sealing capacity of rock salt: a case study of the infra-Cambrian Ara Salt from the South Oman salt basin. AAPG Bulletin 91 (11), 1541–1557.
Schoenherr, J., Schléder, Z., Urai, J.L., Fokker, P.A., Schulze, O., 2007b. Deformation mechanisms and rheology of pre-cambrian rocksalt from the south Oman salt basin. In: Wallner, M., Lux, K., Minkley, W., Hardy, H. (Eds.), Proc. 6th Conference on the Mechanical Behavior of Salt (SaltMech6) – Understanding of THMC Processes in Salt, pp. 167–173.
Schutjens, P.M.T.M., Spiers, C.J., 1999. Intergranular pressure solution in NaCl: grain-to-grain contact experiments under the optical microscope. Oil & Gas Science and Technology 54 (6), 729–750.
Sommaruga, A., 1999. Décollement tectonics in the Jura foreland fold-and-thrust belt. Marine and Petroleum Geology 16, 111–134.
Spiers, C.J., Carter, N.L., 1998. In: Aubertin, M., Hardy, H.R. (Eds.), The Mechanical Behaviour of Salt: Proceedings of the Fourth Conference Series on Rock and Soil Mechanics. Microphysics of rocksalt flow in nature, vol. 22. TTP Trans Tech Publications, Clausthal-Zellerfeld, pp. 115–128.
Spiers, C.J., Schutjens, P.M.T.M., Brezowski, R.H., Peach, C.J., Liezenberg, J.L., Zwart, H.J., 1990. Experimental determination of constitutive parameters govering creep of rocksalt by pressure solution. In: Knipe, R.J., Rutter, E.H. (Eds.), Deformation Mechanisms, Rheology and Tectonics. Geological Society, London, Special Publications, vol. 54, pp. 215–227.
Spötl, C., 1987. Eine klastisch-evaporitische Oberperm-Entwicklung im Hallstätter Salzberg (Salzkammergut, Österreich). Mitteilungen der Österreichischen Geologischen Gesellschaft 80, 115–141.
Spötl, C., 1988. Evaporitische Fazies der Reichenhaller Formation (Skyth/Anis) im Haller Salzberg (Nördliche Kalkalpen, Tirol). Jahrbuch der Geologischen Bundesanstalt 131 (1), 153–168.
Spötl, C., 1989a. The Alpine haselgebirge formation, northern Calcareous Alps (Austria): Permo-Scythian evaporites in an alpine thrust system. Sedimentary Geology 65, 113–125.
Spötl, C., 1989b. Die Salzlagerstätte von Hall in Tirol – ein Überblick über den Stand der geologischen Erforschung des 700jährigen Bergbaubetriebes. In: Veröffentlichungen des Museum Ferdinandeum, Sonderdruck, pp. 137–167.
Spötl, C., 1992. Clay minerals in upper Permian evaporites from the northern Calcareous Alps (Alpines haselgebirge formation, Austria). European Journal of Mineralogy 4, 1407–1419.
Spötl, C., Hasenhüttl, C., 1998. Thermal history of an evaporitic mélange in the northern Calcareous Alps (Austria): a Reconnaissance illite 'crystallinity' and Reflectance study. Geologische Rundschau 87, 449–460.
Spötl, C., Kralik, M., Kunk, M.J., 1996. Authigenic feldspar as an indicator of paleo-Rock/Water Intercalations in Permian Carbonates of the northern Calcareous Alps, Austria. Journal of Sedimentary Research 66 (1), 139–146.
Spötl, C., Kunk, M.J., Ramseyer, K., Longstaffe, F.J., 1998a. Authigenic potassium feldspar: a tracer for the timing of palaeofluid flow in carbonate rocks, northern Calcareous Alps, Austria. In: Parnell, J. (Ed.), Dating and Duration of Fluid Flow and Fluid-Rock Interaction. Geological Society, London, Special Publication No. 144, pp. 107–128.
Spötl, C., Longstaffe, F.J., Ramseyer, K., Kunk, M.J., Wiesheu, R., 1998b. Fluid-rock reactions in an evaporitic mélange, Permian Haselgebirge, Austrian Alps. Sedimentology 45, 1019–1044.
Stöllner, T., 2003. The Economy of Dürrnberg-bei Hallein. An Iron Age salt-mining centre in the Austrian Alps. Antiquaries Journal 83, 123–194.
Ter Heege, J.H., De Bresser, J.H.P., Spiers, C.J., 2005. Dynamic recrystallisation of wet synthetic polycrystalline halite: dependence of grain size distribution on flow stress, temperature and strain. Tectonophysics 396, 35–57.
Tollmann, A., 1987. Late Jurassic/Neocomian Gravitational Tectonics in the Northern Calcareous Alps in Austria. In: Flügel, H.W., Faupl, P. (Eds.), Geodynamics of the Eastern Alps. Deutike, Wien, pp. 112–125.
Trepmann, C.A., Stöckhert, B., 2003. Quartz microstructures developed during non-steady state plastic flow at rapidly decaying stress and strain rate. Journal of Structural Geology 25, 2035–2051.
Trimby, P.W., Drury, M.R., Spiers, C.J., 2000a. Recognising the crystallographic signature of recrystallisation prcesses in deformed rocks: a study of experimentally deformed rocksalt. Journal of Structural Geology 22, 1609–1620.
Trimby, P.W., Drury, M.R., Spiers, C.J., 2000b. Misorientations across etched boundaries in deformed rocksalt: a study using electron backscatter diffration. Journal of Structural Geology 22, 81–89.
Tucker, M.E., 1991. Sedimentary Petrology. An Introduction to the Origin of Sedimentary Rocks, second ed. Blackwell Scientific Publications, Oxford, London et al.
Urai, J.L., Spiers, C.J., Zwart, H.J., Lister, G.S., 1986. Weakening of rock salt by water during long-term creep. Nature 324, 555–557.
Urai, J.L., Spiers, C.J., Peach, C.J., Franssen, R.C.M.W., Liezenberg, J.L., 1987. Deformation mechanisms operating in naturally deformed halite rocks as deduced from microstructural investigations. Geologie en Mijnbouw 66, 165–176.
Urai, J.L., Schléder, Z., Spiers, C.J., Kukla, P.A., 2008. Flow and transport properties of salt rocks. In: Littke, R., Bayer, U., Gajewski, D., Nelskamp, S. (Eds.), Dynamics of Complex Intracontinental Basins. The Central European Basin System. Springer, Berlin et al.
Watanabe, T., Peach, C., 2002. Electrical impedance measurement of plastically deforming halite rocks at 125°C and 50 MPa. Journal of Geophysical Research 107, No. B1, Art. No. 2004.
Wiesheu, R., 1997. Geologisch-geochemische Untersuchungen zur Rekonstruktion der thermischen Geschichte des Haselgebirges. Dissertation. University TU München, Hieronymus, München.
Wiesheu, R., Grundmann, G., 1994. Fluid inclusion studies of anhydrites from the Permo-Skythian beds of the haselgebirge formation (Northern Calcareous Alps, Austria/Germany) International Mineralogical Association, 16th general meeting; Abstracts, 439.
Wise, D.U., Dunn, D.E., Engelder, J.T., 1984. Fault-related rocks – suggestions for terminology. Geology 12, 391–394.